Available online at www.sciencedirect.com
SCIENCE DIRECT®
Journal of Magnetic Resonance 162 (2003) 189–197
JMR Journal of Magnetic Resonance
www.elsevier.com/locate/jmr

An NMR technique for measurement of magnetic field gradient waveforms

Vladimír Jellúš,[a] Jonathan C. Sharp,[b] Boguslaw Tomanek,[b] and Peter Latta[b,*]

[a] *Institute of Measurement Science, Slovak Academy of Sciences, Dúbravská cesta 9, Bratislava SK-84219, Slovakia*
[b] *Institute for Biodiagnostics, National Research Council of Canada, 435 Ellice Avenue, Winnipeg, Man., Canada R3B 1Y6*

Received 29 August 2002; revised 27 February 2003

Abstract

Almost all NMR imaging and localized spectroscopic methods fundamentally rely on the use of magnetic field gradients. It follows that precise information on gradient waveform shape and rise-times is often most useful in experimental MRI. We present a very simple and robust method for measuring the time evolution of a magnetic field gradient. The method is based on the analysis of the NMR signal in the time domain, and requires no specialized field measurement probes for its implementation. The technique makes use of the principal that for small flip angles the excitation profile is a good approximation to the Fourier transform of the radio frequency pulse shape. Creation of the NMR signal can be considered as an inverse Fourier transform and thus variation of the gradient strength during the excitation pulse influences the shape of the NMR signal. Although originally designed for measurement of the rise time only, we have now extended the technique to measure the exact time course of the gradient. The theory is confirmed by experimental results for gradient waveform field measurements in a high-field vertical bore system.

Keywords: Magnetic resonance imaging; Magnetic resonance spectroscopy; Magnetic field gradient; Gradient rise time; Gradient waveform

1. Introduction

Time-varying magnetic field gradients are the primary method used for spatial encoding in magnetic resonance imaging (MRI) experiments. The most common waveforms use a linear ramp to change gradient amplitude. In practice, the gradient field waveform actually generated is not the ideal shape as described digitally, as it is affected by imperfect electronics and power supplies as well as eddy currents induced in conducting material surrounding the gradient coils. Measuring the current flowing through the gradient coils, as a means of monitoring the field may not always be sufficiently accurate as eddy current effects are not taken into account. To get more precise information on time varying gradients the direct measurement of the magnetic field within the magnet bore is preferred.

A number of different techniques have been proposed for gradient waveform measurement. One approach is based upon the measurement of the magnetic field by a pick-up coil [1–3]. The common drawbacks of this technique are: the need for a dedicated, calibrated non-standard electronics and probe; field probes are constructed from electrically conductive materials that may disturb the measured magnetic field; the need for dedicated probes for different sizes of gradient coils and different slew rates; the difficulty in performing accurate measurements in microimaging scanners due to the very limited space.

An alternative solution is to perform the measurements using the NMR signal, namely to observe how the NMR signal is affected by the magnetic field gradient waveform. For example the eddy current field has been studied by measuring the offset frequency of the signal obtained from a small spherical sample [4]. The free induction decays (FIDs) were recorded after various time delays following a gradient pulse and at different physical locations inside the magnet and data were fitted to a sum of decaying exponentials to characterize the eddy currents. Another approach [5] is to measure out-of-phase components of the FIDs detected from small

* Corresponding author. Fax: +204-984-7036.
E-mail address: peter.latta@nrc-cnrc.gc.ca (P. Latta).

1090-7807/03/$ - see front matter
doi:10.1016/S1090-7807(03)00084-3

sample with short relaxation times T_1, T_2. The sequence is easy to implement and is useful for interactive setting of preemphasis compensation network to minimize a shift in the main magnetic field.

Terpstra et al. [6] have demonstrated a method for the measurement of the eddy current effects due to gradient pulses. It is based upon stimulated echoes and projection measurements. Our method differs because it is designed to measure the gradient waveform itself, rather than solely the subsequent eddy current effects.

Balcom at al. [7] proposed a different method for measurement of the gradient waveform. Hard RF pulses were applied at different time points during the rise (or fall) of the gradients and the FIDs were recorded. The gradient time course was then calculated from the width of the phantom profiles, which is dependent on the instantaneous gradient value during excitation of the sample. The precision of this multi-shot method is affected by the uncertainty in the estimation of the width of the measured profiles.

We present another technique for the measurement of the gradient ramp, which relies on the NMR phenomenon only, and does not require specialized field probes and thus can be used in a magnet of any size. The method is very accurate as no extraneous conducting material is placed inside the gradient coils. The method is based on applying rectangular radio frequency (RF) pulse during the gradient rise as shown in Fig. 1. Previously we have presented its first use for the estimation of gradient stabilization time [8]. Additionally we have also shown [9] that this principle can yield gradient time shapes as well. In this paper we present a detailed analysis, theoretical model, and simple experimental measurements of gradient ramp waveforms. The method is in principle a "one shot" technique, however multiple accumulations of the signal increase measurement sensitivity as signal-to-noise (SNR) is improved.

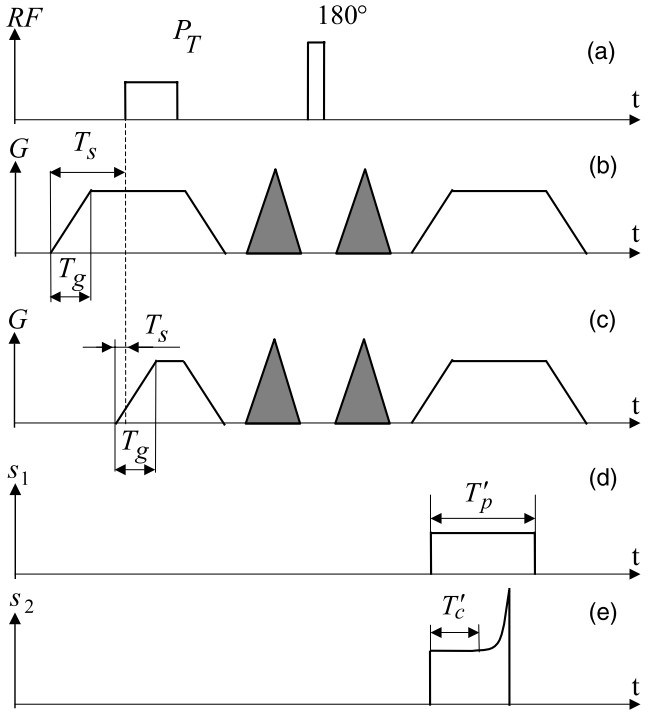

Fig. 1. (a) The spin echo pulse sequence for measurement of the rise time of the gradients; (b) excitation with a constant gradient where the switch time (T_s) is longer than the gradient rise time (T_g); (c) gradient program for the case of excitation during a changing gradient: $T_s < T_g$ (the shaded areas represent trim and spoiler gradients); (d) a typical 'reference' echo signal (constant gradient); (e) a typical 'compressed' echo (variable gradient), where T'_c corresponds to excitation which occurs during constant part of the gradient.

2. Methods

2.1. Theoretical considerations

The proposed gradient waveform measurement can be performed either with a spin-echo or gradient-echo method. The potential problem with gradient echo is its sensitivity to the magnetic field inhomogeneities what can affect the detected signal and thus corrupt the reconstructed gradient waveform. For that reason the spin-echo version of the experimental setup is preferred and will be considered in the following theoretical analysis. For simplicity the relaxation effects on formation of NMR signal are ignored.

The analysis is based on the fact that for a small flip angle, the excitation profile for an RF pulse in the presence of a constant gradient is very similar to the Fourier transform of its envelope with a linear phase shift, see Fig. 1. Consider a sample of infinite extent along the z-axis, with a uniform cross-section. We define the transverse magnetization in the rotating frame as $M_{xy} = M_x + \mathrm{i}M_y$ with a spatially varying precession frequency given as $\omega = \gamma z G$. Let $B_1(t)$ be the amplitude of the applied RF field (magnetic induction (T)) along the axis x of the rotating frame. The transverse magnetization of the spin system, which is initially along the "z" axis $(0, 0, M_0)$, after the RF pulse can be expressed as:

$$M_{xy}(\omega) = K \int_0^T B_1(t) \mathrm{e}^{-j\gamma z \int_t^T G(s)\,\mathrm{d}s} \mathrm{d}t, \tag{1}$$

where $K = j\gamma M_0$ and T is length of the RF pulse [10,11]. For a rectangular RF pulse $P_T(t)$ defined as:

$$P_T(t) = \begin{cases} P, & 0 \leqslant t \leqslant T, \\ 0, & \text{otherwise} \end{cases}$$

and constant gradient G, Eq. (1) can be rewritten as:

$$\begin{aligned} M_{xy}(\omega) &= K e^{-j\omega T} \int_0^T P e^{j\omega t}\,\mathrm{d}t = K \mathrm{e}^{-j\omega T} \mathscr{F}^{-1}\{P_T(t)\} \\ &= K \mathrm{e}^{-j\omega T} M^p_{xy}(\omega), \end{aligned} \tag{2}$$

where $\mathscr{F}^{-1}$ represents the inverse Fourier transform and $M^p_{xy}(\omega)$ is the Fourier transformation of the pulse $P_T(t)$,

i.e., the excitation profile without phase shift. Note that this is true only for small flip angle when $\gamma \cdot P \cdot T \ll 1$ and linear response of the spin system can be assumed. Next consider what happens if we apply a π pulse producing a rotation about the x-axis. The π pulse leaves M_x unchanged, and changes M_y into $-M_y$, i.e., $M_{xy} = M_x - iM_y$ and for transverse magnetization after π pulse can be written as:

$$M_{xy}(\omega) = K^* e^{j\omega T} (M^p_{xy}(\omega))^*, \tag{3}$$

where "*" denotes complex conjugate. The NMR signal is sampled during constant readout gradient G', which has the same sign but in general a different magnitude than the excitation gradient, i.e., $G' = b \cdot G$. Thus the frequency scale is rescaled into $\omega' = b \cdot \omega$ and transverse magnetization into: $M_{xy}(\omega'/b)$. Then the NMR signal can be written as:

$$\begin{aligned} s(t) &= L \int_{-\infty}^{\infty} \left(M_{xy}\left(\frac{\omega'}{b}\right)\right)^* e^{-j\omega' t}\, d\omega' \\ &= LK^* \int_{-\infty}^{\infty} \left(M^p_{xy}\left(\frac{\omega'}{b}\right)\right)^* e^{j(T/b)\omega'} e^{-j\omega' t}\, d\omega', \end{aligned} \tag{4}$$

where L is a complex constant which includes properties of the signal detection channel such as a sensitivity of the receiver coil, amplifier, etc. This integral (Eq. (4)) for the detected signal can be rewritten as:

$$s(t) = LK^*|b| \underbrace{\int_{-\infty}^{\infty} (M^p_{xy}(\omega))^* e^{-j(bt-T)\omega}\, d\omega}_{\mathscr{F}\{(M^p_{xy}(\omega))^*\}}, \tag{5}$$

where $\mathscr{F}$ represents the Fourier transform and $\omega = \omega'/b$. Eq. (2) represents the Fourier relationship between the RF pulse and its excitation profile, whereas Eq. (5) represent the Fourier relationship between the excitation profile and the detected signal. The detected signal can further be written as:

$$s(t) = LK^*|b| \cdot P^*_T(T - b \cdot t). \tag{6}$$

From Eq. (6) it can be seen that detected signal $s(t)$ has a similar shape to the RF pulse $P_T(t)$ but is rescaled in amplitude and length and the time scale is also reversed, i.e., the beginning of the detected signal corresponds to the end of the RF pulse and vice versa. The time reversal arises because the echo is generated from the complex conjugate excitation profile $(M^p_{xy}(\omega))^*$ [12]. For example, if we repeat an experiment and at each repetition the excitation gradient is increased the observed NMR signal becomes lower in amplitude (b is decreasing) and the width of the signal becomes wider.

2.2. Excitation under a time-varying gradient

So far, we have considered excitation and signal acquisition under constant gradients. Now we will examine what happens when excitation is performed during a varying gradient. Suppose, that for small enough time interval $\Delta t = T/M$ the gradient pulse $G(t)$ can be approximated by the step function (Fig. 2):

$$G(t) = \begin{cases} a_0 G_{\text{ref}}, & 0 \leqslant t < \Delta t, \\ a_1 G_{\text{ref}}, & \Delta t \leqslant t < 2 \cdot \Delta t, \\ \vdots & \\ a_k G_{\text{ref}}, & k \cdot \Delta t \leqslant t < (k+1) \cdot \Delta t, \\ \vdots & \\ a_{M-1} G_{\text{ref}} & (M-1) \cdot \Delta t \leqslant t < \Delta t, \end{cases} \tag{7}$$

where M is the total number of the time intervals, and G_{ref} is a constant gradient reference value. Using this gradient approximation the integrals in Eq. (2) can be split into the Δt time intervals during which the gradient is assumed to have a constant value. Then at the end of the RF pulse $P_T(t)$ the transverse magnetization $M_{xy}(\omega)$ can be expressed as:

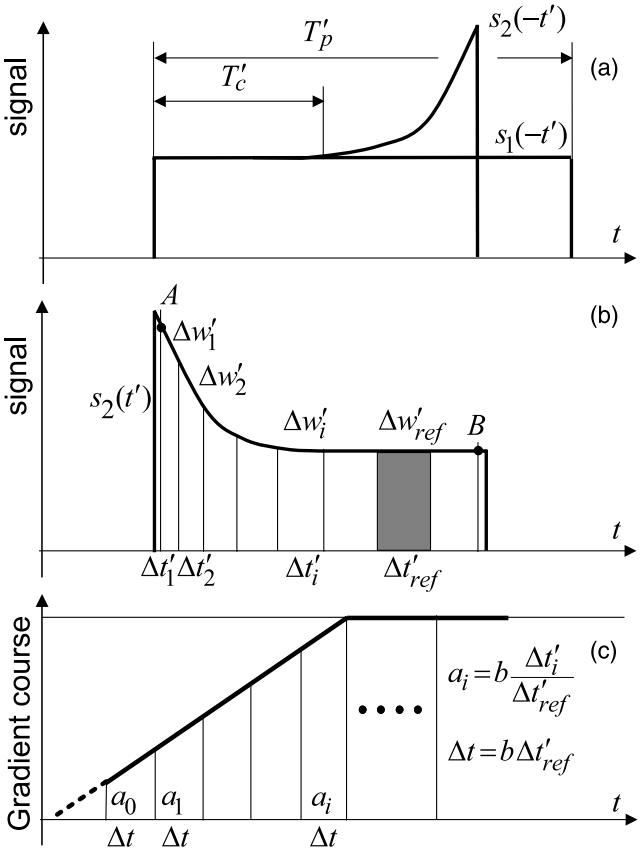

Fig. 2. Illustration of the reconstruction of the gradient shape from the time-reversed compressed echo: (a) the reference and compressed echo signals. The gradient rise time can be calculated from T'_p and T'_c; (b) the compressed echo between points A and B is divided into intervals $\Delta w'_i$, each of equal area $\Delta w'_{\text{ref}}$; (c) the intervals ($\Delta t'_i$) are used to calculate the gradient amplitude coefficients a_i.

$$M_{xy}(\omega)=\sum_{k=0}^{M-1}\left[K\int_{k\Delta t}^{(k+1)\Delta t}P\exp\left\{-j\gamma z\left(a_kG_{\mathrm{ref}}\int_t^{(k+1)\Delta t}\mathrm{d}s+\sum_{l=k+1}^{M-1}\left(a_lG_{\mathrm{ref}}\int_{l\Delta t}^{(l+1)\Delta t}\mathrm{d}s\right)\right)\right\}\mathrm{d}t\right] \tag{8}$$

thus calculating integrals in the exponent:

$$M_{xy}(\omega)=\sum_{k=0}^{M-1}\left[K\int_{k\Delta t}^{(k+1)\Delta t}P\exp\left\{-j\gamma z\left(a_kG_{\mathrm{ref}}(k+1)\Delta t-a_kG_{\mathrm{ref}}t+\sum_{l=k+1}^{M-1}a_lG_{\mathrm{ref}}\Delta t\right)\right\}\mathrm{d}t\right]. \tag{9}$$

Substitution of the variable t in the exponent by $t+k\Delta t$ and a corresponding change of integration limits gives:

$$\begin{aligned}M_{xy}(\omega)&=\sum_{k=0}^{M-1}K\left[\int_0^{\Delta t}P\exp\left\{-j\gamma z\left(a_kG_{\mathrm{ref}}(k+1)\times\Delta t.-a_kG_{\mathrm{ref}}(t+k\Delta t)+\sum_{l=k+1}^{M-1}a_lG_{\mathrm{ref}}\Delta t\right)\right\}\mathrm{d}t\right]\\&=\sum_{k=0}^{M-1}K\left[\exp\left\{-j\gamma z\sum_{l=k}^{M-1}a_lG_{\mathrm{ref}}\Delta t\right\}\int_0^{\Delta t}P\exp\left\{j\gamma za_kG_{\mathrm{ref}}t\right\}\mathrm{d}t\right].\end{aligned} \tag{10}$$

Introducing a rectangular RF pulse $P_{\Delta t}(t)$ defined as:

$$P_{\Delta t}(t)=\begin{cases}P, & 0\leqslant t\leqslant\Delta t,\\ 0, & \text{otherwise}\end{cases}$$

and using $\omega_{\mathrm{ref}}=\gamma zG_{\mathrm{ref}}$, the transverse magnetization (in the presence of a variable gradient) at the end of the rectangular RF pulse $P_T(t)$ can be written as:

$$M_{xy}(\omega)=\sum_{k=0}^{M-1}K\left[\exp\left\{-j\sum_{l=k}^{M-1}a_l\omega_{\mathrm{ref}}\Delta t\right\}\times\underbrace{\int_{-\infty}^{\infty}P_{\Delta t}(t)\mathrm{e}^{ja_k\omega_{\mathrm{ref}}t}\mathrm{d}t}_{m_{xy}^p(a_k\omega_{\mathrm{ref}})=\mathscr{F}^{-1}\{P_{\Delta t}(t)\}}\right]. \tag{11}$$

Eq. (11) shows that final transverse magnetization produced by a rectangular pulse $P_T(t)$ and variable gradient $G(t)$ can be expressed as the sum of the rescaled partial excitation profiles $m_{xy}^p(a_k\omega_{\mathrm{ref}})$ of RF pulses $P_{\Delta t}(t)$. Each of these profiles is multiplied by a complex constant $\exp\{-j\sum_{l=k}^{M-1}a_l\omega_{\mathrm{ref}}\Delta t\}$, which holds information about the remaining gradient waveform after excitation of this profile and is unique for each profile. These profiles are now rescaled just in the frequency domain, while the magnitude remains unchanged. Now, we have to again consider the effect of the refocusing π pulse, which rotate transverse magnetization around x-axis. The transverse magnetization after the π pulse can be written as:

$$M_{xy}(\omega)=\sum_{k=0}^{M-1}K^*\left[\exp\left\{j\sum_{l=k}^{M-1}a_l\omega_{\mathrm{ref}}\Delta t\right\}(m_{xy}^p(a_k\omega_{\mathrm{ref}}))^*\right] \tag{12}$$

which indicates that the transverse magnetization is now equal to the complex conjugate of the excitation profile.

2.3. Acquisition gradient

Let us further apply an acquisition gradient G', i.e., $G'=bG_{\mathrm{ref}}$ and $\omega'=b\cdot\omega_{\mathrm{ref}}$. Then from Eqs. (4) and (12), the acquired signal can be expressed as:

$$s(t)=L\int_{-\infty}^{\infty}\left[\sum_{k=0}^{M-1}K^*\left[\exp\left\{j\sum_{l=k}^{M-1}\frac{a_l}{b}\omega'\Delta t\right\}\left(m_{xy}^p\left(\frac{a_k}{b}\omega'\right)\right)^*\right]\right]\mathrm{e}^{-j\omega' t}\mathrm{d}\omega'. \tag{13}$$

Applying the linear property (addition theorem) of the Fourier transform [12], terms in the sum can be transformed separately and the results combined, i.e. integration and summation in Eq. (13) can be exchanged. Thus the signal corresponding to the kth member is given by:

$$\begin{aligned}s_k(t)&=LK^*\int_{-\infty}^{\infty}\left(m_{xy}^p\left(\frac{a_k}{b}\omega'\right)\right)^*\times\exp\left\{j\sum_{l=k}^{M-1}\frac{a_l}{b}\omega'\Delta t\right\}\mathrm{e}^{-j\omega' t}\mathrm{d}\omega'=LK^*\left|\frac{b}{a_k}\right|\\&\times\underbrace{\int_{-\infty}^{\infty}(m_{xy}^p(\omega))^*\exp\left\{-j\frac{1}{a_k}\left(b\cdot t-\sum_{l=k}^{M-1}a_l\Delta t\right)\omega\right\}\mathrm{d}\omega}_{\mathscr{F}\{(m_{xy}^p(\omega))^*\}},\end{aligned} \tag{14}$$

where $\omega=(a_k/b)\omega'$. Applying a Fourier transformation to the partial excitation profiles $(m_{xy}^p(\omega))^*$ the relationships between kth excitation pulse $P_{\Delta t}(t)$ and corresponding signal response can be found:

$$s_k(t)=LK^*\left|\frac{b}{a_k}\right|\cdot P_{\Delta t}^*\left(\frac{1}{a_k}\left(\sum_{l=k}^{M-1}a_l\Delta t-b\cdot t\right)\right) \tag{15}$$

or for the whole pulse $P_T(t)$ the sampled signal is as follows:

$$s(t)=LK^*\sum_{k=0}^{M-1}\left|\frac{b}{a_k}\right|\cdot P_{\Delta t}^*\left(\frac{1}{a_k}\left(\sum_{l=k}^{M-1}a_l\Delta t-b\cdot t\right)\right). \tag{16}$$

From Eq. (16) the following conclusions concerning the detected signal can be drawn:

1. The negative sign of the time variable means that the time axis of the detected signal is reversed, when compared to the time axis of the excitation pulse. In other words, what happens at the beginning of excitation is reflected at the end of the signal and vice versa.

2. The detected signal can be represented by a sum of rectangular pulses. Each of these pulses has a rescaled magnitude and duration, which depend upon the ratio of the readout and corresponding excitation gradient (instantaneous gradient value $a_k G_{\mathrm{ref}}$).
3. Each pulse is shifted from the beginning of the signal by the sum of the lengths of all the previous pulses.

In the next section we will use these relationships between excitation profile, gradient strength, and detected signal to design the measurement pulse sequence and an algorithm for gradient shape calculation.

2.4. Pulse sequence

The pulse sequence proposed for gradient rise time measurement is shown in Figs. 1a–c. The spin-echo experiment was chosen, because it is less sensitive to B_0 inhomogeneity and therefore T_2^* decay when compared to the gradient-echo. The spin excitation is performed by a rectangular, low flip angle RF pulse $P_T(t)$ in the presence of the gradient under examination. The sequence is implemented to allow adjustment of the gradient switch time T_s, i.e., the time delay between gradient onsets and beginning of the $P_T(t)$ pulse. The gradients placed around the refocusing 180° RF pulse function as trim and spoiler gradients. The echo signal is sampled with constant readout gradient pulse. When the length of the excitation RF pulse $P_T(t)$ is set longer than the gradient rise time T_{g}, i.e., $T > T_{\mathrm{g}}$, then the value of the T_s parameter determines the behavior of the spin excitation and which of two types of echoes can be observed.

Reference echo. When the delay between the beginning of the gradient pulse and the beginning of the RF pulse (T_s) is much longer than the gradient rise time, i.e., $T_s > T_{\mathrm{g}}$, the gradient has enough time to stabilize and excitation is performed with constant gradient (Figs. 1a and b). The detected NMR signal has a rectangular shape similar to the excitation RF pulse (echo s_1 in Fig. 1d) but with a rescaled length T'_p given by the ratio of the readout and excitation gradient amplitudes, due to Eq. (6). This signal will be called the *reference* echo and can be used as the reference data.

Compressed echo. When $T_s < T_{\mathrm{g}}$, some part of the spin excitation is performed during the gradient ramp (Figs. 1a–c). In this case a change of the signal envelope can be observed and the typical echo shape for such case is shown in Fig. 1e. The part of the signal that corresponds to the excitation during the gradient ramp is compressed in time and increased in magnitude due to Eq. (16). We refer to this as the *compressed* echo and the switch time as T_{s_2}.

2.5. Calculation of gradient rise time

The simplest task is to determine the gradient rise time, i.e., the time needed for the gradient to reach the required amplitude. This time can be calculated by comparing the reference and compressed echoes, Fig. 2a. The reference echo allows determination of the stable part of the compressed echo. The gradient rise time T_{g} is given by:

$$T_{\mathrm{g}} = b \cdot \left(T'_p - T'_c\right) + T_{s_2} \tag{17}$$

where T'_p is the length of the reference echo, T'_{c} is the constant part of the compressed echo, b is rescaling factor from Eq. (6) and T_{s_2} is the gradient switch time.

2.6. Gradient shape reconstruction algorithm

The compressed echo can be used not only for gradient rise time calculation but also for reconstruction of the full gradient shape. This could be particularly useful when the gradient shape is more complicated than a simple ramp and the knowledge of the exact gradient shape is desirable. The principle of gradient shape reconstruction is based on Eq. (16), namely that the compressed echo contains information about the gradient magnitude time course and can be represented by a sum of rectangular pulses. Thus calculation of the coefficients a_k from the compressed echo allows gradient shape to be determined. This is illustrated in Figs. 2b and c and includes the following steps (Fig. 2):

1. Calculate the modulus of the detected signal.
2. Reversal of the time axis of the acquired compressed echo $s_2(-t')$—the signal is flipped in the left-right direction (Fig. 2b).
3. Selection of the bounds (A, B) of the compressed echo $s_2(t')$ on which the calculation will be performed (Fig. 2b).
4. Determination of the reference value $s_2(t'_{\mathrm{ref}})$ from the part of the signal where the gradient is assumed to be already constant and thus calculate the reference area as:
$$\Delta w'_{\mathrm{ref}} = s_2(t'_{\mathrm{ref}}) \cdot \Delta t'_{\mathrm{ref}}, \tag{18}$$
where $\Delta t'_{\mathrm{ref}}$ is the length of the reference interval.
5. Division of the interval between points A and B into intervals $\Delta t'_i$ in such way that area under the signal $s_2(t')$ on the each of these intervals is equal to the reference area $\Delta w'_{\mathrm{ref}}$.
6. Calculation of the coefficient a_i and time interval Δt as follows:
$$\Delta t = b\Delta t'_{\mathrm{ref}}, \tag{19}$$
$$a_i = b\frac{\Delta t'_i}{\Delta t'_{\mathrm{ref}}}. \tag{20}$$
7. Reconstruction of the gradient shape from the calculated coefficients a_i and Δt using Eq. (7).

Besides the electronic random noise, there are some experimental factors that limit the accuracy of the echo shape calculations. The receiver dynamic range and the bandwidth of the receiver low-pass filter ultimately limit

the height and sharpness of the peak at the end of the echo. Additionally at low gradient values (i.e., at the beginning the ramp) the RF pulse excites a larger extent of the sample, and thus sample edge effects (i.e., shape and size) can affect the received signal.

Due to these effects the total area of the compressed echo cannot be used for gradient shape calculation. Both ends of the echo, which are mostly affected by these effects, have to be excluded from calculation, and reconstruction can be done only on the interval (A, B). This, together with the use of a finite switch time T_s between measured gradient onset and the RF pulse,set limits on the reconstruction of the very beginning of the gradient ramp. Consequently the very start of the gradient lobe can be only be estimated, e.g., by extrapolation. Note that whereas the reconstructed gradient waveform time scale is accurate, being the same as the time scale of the measured echo, the gradient magnitude is in arbitrary units since it depends upon the arbitrarily scaled echo signal amplitude.

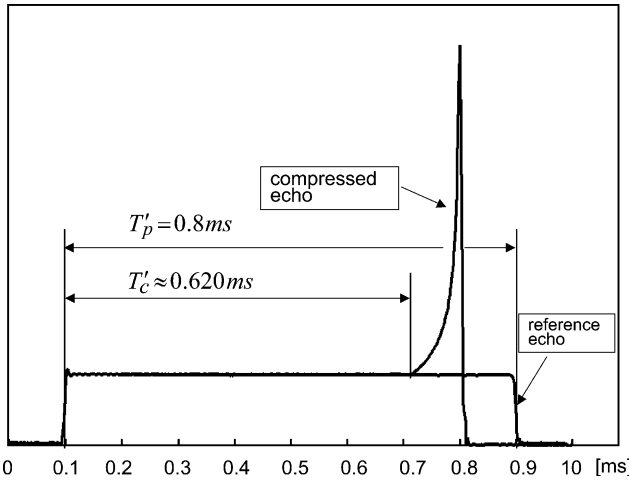

Fig. 3. Experimentally obtained reference and compressed echo signals (displayed as modulus). The gradient amplitude was 80 mT/m for both excitation and readout gradient, i.e., $b = 1$. The reference echo length was $T'_p = 0.8$ ms and the estimated constant part of the compressed echo is $T'_c \approx 0.620$ ms. The calculated gradient rise time is $T_g = 0.19$ ms.

3. Experimental methods

All experiments were carried out using 11.7 T, 7 cm vertical bore magnet (Magnex UK) equipped with self-shielded gradient system SGRAD123/72/S and Techron gradient amplifiers 7300 Series. The spectrometer was an Avance DRX Bruker console (Bruker, Kalsruhre, Germany). A 2 cm i.d. Helmholtz coil was employed in all experiments. Two types of phantoms were used: a plastic tube (inner diameter 1.4 cm and length 5 cm) and a spherical glass vessel (inner diameter 2.2 cm). Both were filled with $CuSO_4$ doped water with $T_1 = 370$ ms and $T_2 = 240$ ms. The tube was oriented along the measured gradient field direction. The sphere phantom made experiments more convenient and faster because orientation of the phantom did not have to be changed for different gradients. A rectangular RF pulse with flip angle about 11° and duration 800 μs was employed for spin excitation. The length of the 180° refocusing hard pulse was 100 μs. All experiments were done with the same parameters: echo time (TE) 3.36 ms, time repetition (TR) 2 s, and 32 averages. The length of the data acquisition was 1.024 ms during which 512 complex sample points were acquired. Six dummy scans were used before each data acquisition to reach steady state. The total experiment time for each data acquisition was approximately 76 s. In all experiments the gradient under examination was ramped from zero to 80 mT/m in 175 μs.

4. Results and discussion

Fig. 3 shows the reference and compressed echoes from the Z gradient measurements using the tube phantom. The length of the reference echo (T'_p) is 0.8 ms and the length of the stable part of the compressed echo (T'_c) was estimated to be about 0.620 ms. The gradient switch time T_{s_2} was 0.01 ms and the readout/excitation gradient ratio (b) was unity. Using Eq. (17) the gradient rise time (T_g) was estimated to be 0.190 ms.

Time dependent gradient behavior was examined more closely by using the gradient shape reconstruction algorithm. Setting the bounds (A, B) and choosing the reference values from the constant echo part was done manually (point 3 and 4 of the algorithm). The length of the reference interval $\Delta t'_{\text{ref}}$ was equal to the sampling interval, i.e., 2 μs. When the echo was divided into parts with equals areas (point 5 of the algorithm) a cubic spline interpolation [13] was used to calculate signal values between samples. The results of gradient calculations are shown in Fig. 4. together with the measured gradient amplifier currents for each coil. The calculated gradient ramps are shown beginning at a point about 30% up the ramp. The missing points were extrapolated by a linear fit. The beginning of the gradient pulse was then estimated as the crossing point of this line with the time axis.

Comparing the reconstructed gradient ramps from the tube and sphere phantoms, it can be seen that the data from sphere exhibit ripples distortions. This is particularly visible for the X and Y gradients. The most likely cause was imperfect centering of the sphere phantom in the X and Y-axes. Along the Z-axis positioning of the sphere phantom was very accurate, thus both the reconstructed gradient shapes were almost identical.

Comparison of the measured gradients waveforms with the gradient amplifier current monitor shows good

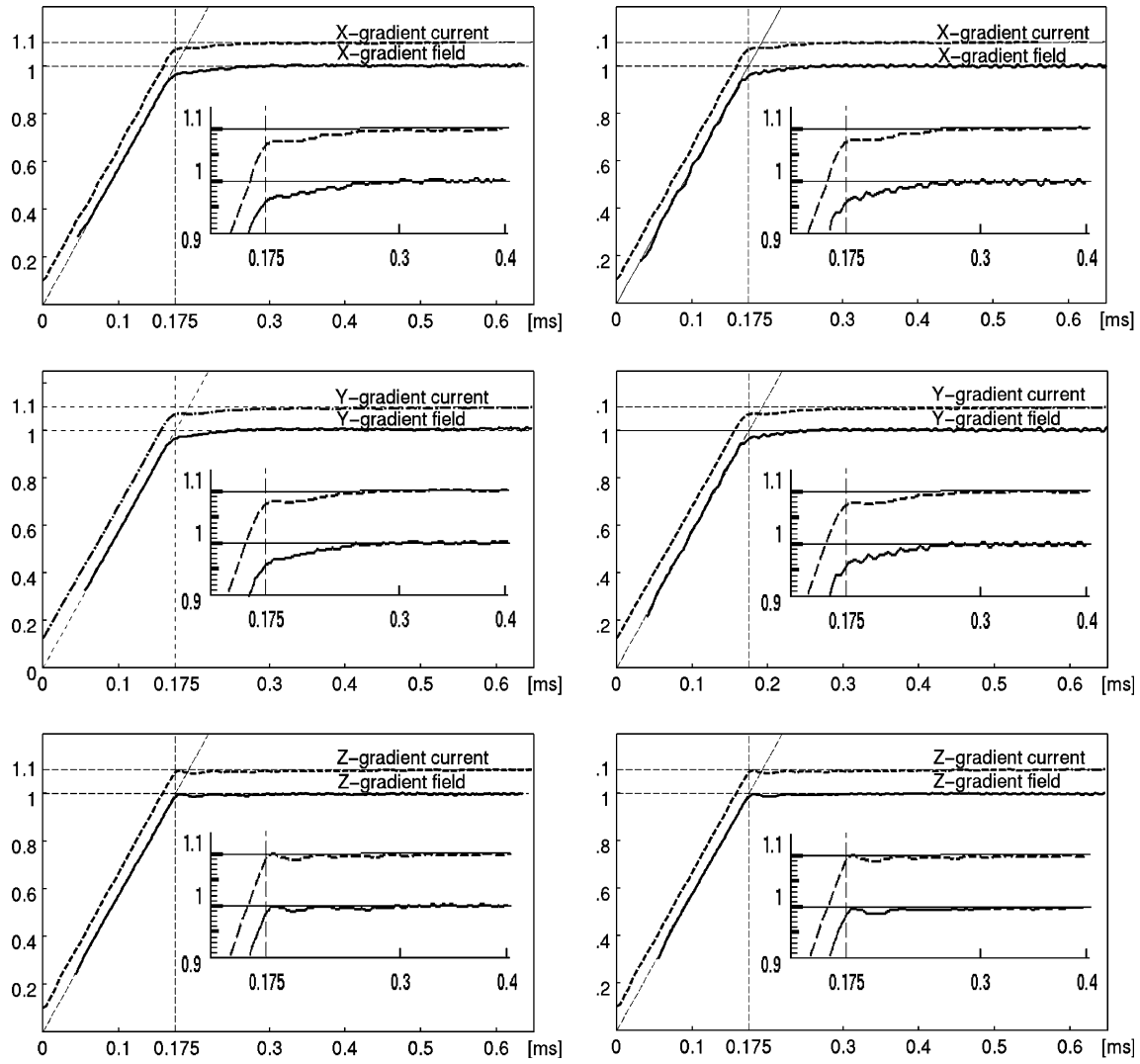

Fig. 4. Results of gradient shape reconstruction (solid lines) compared to measured gradient currents (dashed lines and plotted shifted up 10% for clarity) for X, Y, and Z gradients (top, middle, bottom). Data from the tube phantom and sphere phantom are shown in the left and right columns, respectively. The X and Y reconstructions exhibit ripples distortions, most likely caused by slightly off-center position of the sphere phantom in X and Y-axes. The magnified part of the reconstructed gradient is shown for revealing fine details.

agreement. This might indicate that for this particular gradient system the more serious problem is the inductance of the gradient coils themselves rather than eddy currents. The X and Y gradients coils, which produce the more corrupted gradient ramp, have inductance 177 μH. This is twice the value of the Z gradient coil inductance (83 μH).

The performance of the method is mainly determined by two factors: signal-to-noise ratio of the acquired signal and the limited extent of the sample along the measured gradient. Signal-to-noise ratio can be improved by increased signal averaging at the expense of a longer measurement time. The sample length is limited by the size of the RF coil and/or the size of the imaging volume. A limited sample length equates to a limited signal frequency bandwidth, which is manifested as a ringing artifact (Gibbs phenomenon) and/or edge smoothing at both ends of the echo. This edge smoothing is more noticeable when low gradient amplitudes and a small sample size are used. By using a sample that is longer than the coil this effect is minimized. This strategy has the additional advantage that the coil spatial sensitivity acts as a smoothing window and helps to partially suppress ringing artifacts. Due to this effect low gradient values at the beginning or end of a gradient pulse cannot be reconstructed from the experimental signal.

In order to estimate the impact of the edge effect on the precision of the gradient reconstruction we did reference measurement for the stabilized gradient amplitude (see Figs. 1a and b). The precision of the gradient amplitude calculation and changes in echo area were examined for particular gradient amplitudes. Two-reference datasets were acquired with the plastic tube

Table 1
Calculation of the gradient amplitude from reference echo to estimate impact of the finite sample length on the precision of reconstructed gradient shape

Gradient amplitude in (%)[a]	Readout gradient amplitude					
	20 mT/m			80 mT/m		
	Relative echo area in (%)[b]	Calculated gradient amplitude in (%)[c]	Relative error of the calculated gradient in (%)[d]	Relative echo area in (%)[b]	Calculated gradient amplitude in (%)[c]	Relative error of the calculated gradient in (%)[d]
50	101.428	49.3	0.717	102.642	49.3	0.747
75	100.837	74.5	0.508	101.799	74.1	0.909
80	100.537	79.6	0.353	101.508	79.2	0.804
90	100.412	89.7	0.282	100.811	89.5	0.497
100	100	—	—	100	—	—

[a] Gradient amplitude (in percent of readout gradient).
[b] Relative echo area (in percent of echo area for 100% gradient amplitude) calculated from modulus of the experimental signal.
[c] The amplitude has been calculated from 100 samples taken from the echo center to minimize random error.
[d] Relative error of the calculated gradient amplitude.

positioned along the Z-axis and using 20 and 80 mT/m readout gradient amplitudes. The amplitude of measured gradient was set for 50, 75, 80, 90, and 100% (i.e., $b = 2$, 1.33, 1.25, 1.11, and 1) of readout gradient for each dataset. The gradient switch time was set at $T_s = 100$ ms to minimize any eddy current effects on the reference echo. All remaining parameters were identical as in the previous experiments, i.e., TE = 3.36 ms, time repetition TR = 2 s and 32 averages. From each dataset two parameters were calculated: total echo area and the relative gradient amplitude relative to readout gradient. To minimize random errors the gradient amplitude was estimated from 100 points taken from the center of the echo. The results are summarized in Table 1 and reveal that: echo area differences between half- and full-amplitude of the excitation gradient were less than 3%; the calculation of the gradient amplitude had less than 1% error for all measurements. This indicates that error during gradient shape reconstruction caused by the finite sample length was about 1% of the full gradient pulse magnitude.

A natural question, which arises here, is whether the method is capable of detecting induced eddy currents during the gradient switching. It should be noted that induced time-varying magnetic fields have two main components: a magnetic field gradient opposite to the applied gradient and a B_0 shift in the main magnetic field. The proposed method in principal is sensitive only to the first component and is not sensitive to B_0 shifts of the main magnetic field, which must be measured with another technique, e.g. [5]. The estimated precision indicates that it can be used for monitoring the eddy current of the order of 1% at gradient peaks. However the method is not suitable for measuring eddy current effects at low gradient values.

A unique feature of the proposed method is that it provides the shape of the measured gradient waveform. Although, a similar feature has been reported previously [7], our approach has the potential to be much more precise and more convenient for use because the previous method measures the gradient waveform in discrete selected points and for each point a separate measurement is performed. With such a method small gradient glitches (as shown in Fig. 4 for Z-gradient) might be overlooked. Another problem, reported with the previous method, was that reconstruction of the gradient waveform was affected by uncertainty of the measured profile.

5. Conclusions

We have presented an NMR method for direct measurement of the temporal evolution of magnetic field gradients. The main advantage of this technique is that it does not require any additional hardware. In fact it is based on the same principles that are used for MRI, and thus can be used for measurements in MRI scanners of any size. We have proved that this technique can yield results that correspond very precisely to the measurement of current flowing through gradient coils. A main application area is the testing of gradient system components (power amplifiers, filters, cables, and coils).

Another application is the measurement of aspects of eddy current behavior, in particular the eddy current gradient fields when the gradient is on (e.g., at a nominal plateau). The method is not suitable for measurement of small residual gradients when the gradient is nominally off, nor for measurement of shifts of the main B_0 magnetic field induced by gradient switching. Practical experience has shown that the method can be successfully used with high-field gradients as well as with spectrometers with substantially lower gradients field, e.g., 20 mT/m as has been reported in [8,9].

References

[1] J. Chankji, J.L. Lefevre, A. Briguet, A method for mapping magnetic fields generated by current coils, J. Phys. E 18 (1985) 1014–1017.

[2] D.J. Jensen, W.W. Brey, J.L. Delayre, P.A. Narayana, Reduction of pulsed gradient settling time in the superconducting magnet of a magnetic resonance instrument, Med. Phys. 14 (1987) 859–862.

[3] V. Senaj, G. Guillot, L. Darrasse, Inductive measurement of magnetic field gradients for magnetic resonance imaging, Rev. Sci. Instrum. 69 (1998) 2400–2405.

[4] S. Robertson, D.G. Hughes, Q. Liu, P.S. Allen, Analysis of the temporal and spatial dependence of the eddy current fields in a 40-cm bore magnet, Magn. Reson. Med. 25 (1992) 158–166.

[5] R.E. Wysong, I.J. Lowe, A simple method of measuring gradient induced eddy currents to set compensation networks, Magn. Reson. Med. 29 (1993) 119–121.

[6] M. Terpstra, P.M. Andersen, R. Gruetter, Localized eddy current compensation using quantitative field mapping, J. Magn. Reson. 131 (1998) 139–143.

[7] B.J. Balcom, M. Bogdan, R.L. Armstrong, Single-point imaging of gradient rise, stabilization, and decay, J. Magn. Reson. A 118 (1996) 122–125.

[8] V. Jellúš, P. Latta, L. Budinsky, I. Tkáč, J. Coremans, R. Luypaert, A simple "One shot" method for measuring the rise time of gradients, in: Proceedings of the 4th Annual Meeting of ISMRM, New York, 1996, p. 1387.

[9] V. Jellúš, P. Latta, L. Budinsky, I. Tkáč, J. Coremans, R. Luypaert, A Simple "One shot" method for measuring the time course of gradients, in: Book of Abstract in Magnetic Resonance Materials in Physics, Biology, and Medicine, vol. 4, Prague, 1996, p. 270.

[10] J. Pauly, D. Nishimura, A. Macovski, A *k*-space analysis of small-tip-angle excitation, J. Magn. Reson 81 (1989) 43–56.

[11] P.G. Morris, Frequency selective excitation using phase-compensated RF pulses in one and two dimensions, in: P. Diehl, E. Fluck, H. Günther, R. Kosfeld, J. Seelig (Eds.), NMR Basic Principles and Progress, vol. 26, Springer-Verlag, Berlin, 1992, pp. 149–170.

[12] R.N. Bracewell, The basic theorems, in: The Fourier Transform and its Applications, McGraw-Hill, New York, 1999, pp. 105–135.

[13] W.H. Press, S.A. Teukolsky, W.T. Vetterling, B.P. Flannery, Interpolation and extrapolation, in: Numerical Recipes in C, Cambridge University Press, Cambridge, 1992, pp. 105–128.